Andriy CZABAN[1,2], Marek LIS[1]

Częstochowa University of Technology, Faculty of Electrical Engineering (1); Lviv University of Technology, Chair of Mechanics (2)

Mathematical modelling of transient states in a drive system with a long elastic element

Streszczenie. *W pracy przedstawiono model matematyczny głębokożłobkowego napędu asynchronicznego z długim elementem sprężystym. System rozpatrywano jako układ o elektrycznych i mechanicznych parametrach rozłożonych. Dla opracowania różniczkowych równań stanu wykorzystano nawą interdyscyplinarną metodę, która bazuje się na modyfikacji zasady Hamiltona-Ostrogradskiego. Na podstawie modelu poddano analizie stany nieustalone pracy układu napędowego z silnikiem głębokożłobkowym. Wyniki symulacji komputerowej przedstawiono w postaci graficznej. (**Model matematyczny głębokożłobkowego napędu asynchronicznego z długim elementem sprężystym**)*

Summary. *In the paper a mathematical model of a deep-slot asynchronous drive with an elastic element is presented. The system is considered as having distributed electrical and mechanical parameters. In order to derive differential state equations a novel interdisciplinary approach was used, based on a modification of Hamilton-Ostrogradsky principle. On the basis of the model the transient states of the drive system with deep slot motor were considered. The results of computer simulations were presented in the graphical form.*

Słowa kluczowe: zasada Hamiltona, Euler-Lagrange'a system, napęd głębokożłobkowy, długi element sprężysty
Keywords: Hamilton's principle, Euler-Lagrange's system, deep slot drive, long elastic elements

Introduction

In the paper a mathematical model of an asynchronous drive with a long elastic shaft line with deep slot motor was considered. In the classical long shaft lines of asynchronous drives are usually considered as connections of elementary mechanical units [2]. Such approach in the general case does not sufficiently refer to fundamental physical approaches, in particular for nonlinear system parameters. In order to avoid this, a mathematical model of shaft line was proposed as a system of distributed electrical and mechanical parameters. Also, in order to avoid decomposition of the complex electromechanical system, in the present work the mathematical model of the asynchronous drive is developed on the basis of novel interdisciplinary variational principle, which is based on an extension of Hamilton-Ostrogradsky principle to nonconservative dissipative non-autonomous systems using a modification of the well-known Lagrange's function [1]. It means that the mathematical models of these devices are described with differential equations with ordinary and partial derivatives.

Therefore, the aim of the paper is to obtain a mathematical model of a deep-slot asynchronous drive with a long elastic shaft line, on the basis of variational principles. Also the analysis of transient electrical and mechanical states on the basis of the developed model is considered.

Mathematical model of the system.

Mathematical model of the electromechanical system obtained with the use of variational methods is presented [1, 4]. In the analyzed example an electric drive has been presented. It consists of a deep slot asynchronous motor, which rotates the mechanism of active load with an assumed value of inertia moment through a long elastic shaft (Fig. 1)

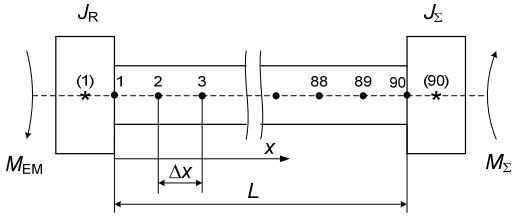

Fig. 1. A graph of an asynchronous drive

For the electromechanical system (Fig. 1) the components of Lagrangian are presented [1]

$$\tilde{T}^* = \sum_{i=1}^{3}\int_0^{i_{Sj}} \Psi_{Sj}(i_{Sj})di_{Sj} + \sum_{j=1}^{3}\int_0^{i_{Rj}} \Psi_{Rj}(i_{Rj})di_{Rj} + \frac{J_{EM}\omega_1^2}{2} +$$

(1) $$+\frac{J_\Sigma\omega_{90}^2}{2};\quad T = \frac{\rho J_p}{2}\left(\frac{\partial\varphi}{\partial t}\right)^2;\quad P = \frac{GJ_p}{2}\left(\frac{\partial\varphi}{\partial x}\right)^2;$$

(2) $$\Phi^* = \frac{1}{2}\int_0^t\sum_{j=1}^{3}\left(r_{Sj}i_{Sj}^2 + r_{RLj}i_{Rj}^2\right)d\tau;\quad \Phi = \xi\left(\frac{\partial^2\varphi}{\partial x\partial t}\right)^2;$$

$$D^* = \int_0^t\sum_{j=1}^{3}\left(u_{Sj}i_{Sj} - u_{Rj}i_{Rj}\right)d\tau + \int_0^t\int_0^{\omega_1} M_{EM}\,d\omega_1 d\tau -$$

(3) $$\int_0^t\int_0^{\omega_{90}} M_\Sigma\,d\omega d\tau,\quad j = A,B,C,$$

where $\tilde{T}^*$ – kinetical coenergy, P^* – potential energy, Φ^* – dissipation energy, D^* – energy of external, T,P,Φ,D – densitites of the aforementioned functions, M_{EM} – elektromagnetic moment of the motor, M_Σ – load moment of the drive, J_Σ – total inertia moment of the electric drive, S,R – indexes for reference to stator and rotor, respectively, Q – charge in the circuit, $i = \dot{Q}$ – current in the circuit, Ψ – total magnetic coupling, r_S – resistance of stator winding, r_{RL} – resistance of rotor head part, u_S – phase voltage of motor supply, u_R – voltage in bars of rotor cage, $\varphi(x,t)$ – shaft return angle, $\omega = \partial\varphi/\partial t$ – angular velocity of shaft, τ – additional integration variable, G – module of transverse elasticity, ξ – coefficient of internal dissipation in the shaft, x – current coordinate along the shaft, ρ – density of shaft material, J_p – polar inertial moment of the shaft, $\mathbf{q} \equiv (Q_{SA}, Q_{SB}, Q_{SC}, Q_{RA}, Q_{RB}, Q_{RC})^{\mathrm{T}}$;

$\dot{\mathbf{q}} \equiv (i_{SA}, i_{SB}, i_{SC}, i_{RA}, i_{RB}, i_{RC})^{\mathrm{T}}$ – generalized coordinates and velocities.

The variation of action functional [1] is gives as

$$\delta S = \delta \int_0^{t_1} \left(L^* + \int_l L dl \right) dt = \int_0^{t_1} \delta L^* dt + \int_0^{t_1} \int_l \delta L dl dt \,. \tag{4}$$

where L^* – modified Lagrange's function, L – linear density of the modified Lagrange's function [1, 2].

The variation of action functional according to Hamilton will be equal to zero only in the case, when the dynamical system is described with Euler-Lagrange's equations [2]

$$\frac{d}{dt}\frac{\partial L^*}{\partial \dot{q}_s} - \frac{\partial L^*}{\partial q_s} = 0 \,, \tag{5}$$

where $L^* = T^* - P^* + \Phi^* - D^*$
and with Euler-Poisson equation [1, 4]

$$\frac{\partial L}{\partial q} - \frac{\partial}{\partial x}\frac{\partial L}{\partial q_x} + \frac{\partial^2}{\partial x \partial t}\frac{\partial L}{\partial q_{xt}} - \frac{\partial}{\partial t}\frac{\partial L}{\partial q_t} = 0 \,, \tag{6}$$

where $L = T - P + \Phi - D$.

Substituting Lagrangians L^* into Equation (5), and L into Equation (6):

$$i_{SA} + i_{SB} + i_{SC} = 0, \quad i_{RA} + i_{RB} + i_{RC} = 0 \,; \tag{7}$$

$$\psi_{SA} + \psi_{SB} + \psi_{SC} = 0, \quad \psi_{RA} + \psi_{RB} + \psi_{RC} = 0 \,; \tag{8}$$

$$\mathbf{\Psi}_S = \mathbf{L}_{\sigma S}\mathbf{i}_S + \boldsymbol{\psi}_S, \quad \mathbf{\Psi}_R = \mathbf{L}_{\sigma RL}\mathbf{i}_R + \boldsymbol{\psi}_R \,; \tag{9}$$

$$\boldsymbol{\psi}_S \equiv \boldsymbol{\psi} = \mathbf{\Pi}^{-1}\boldsymbol{\psi}_R, \ \mathbf{L}_{\sigma S}^{-1} = \boldsymbol{\alpha}_{\sigma S}, \ \mathbf{L}_{\sigma RL}^{-1} = \boldsymbol{\alpha}_{\sigma RL} \,, \tag{10}$$

where ψ – fundamental magnetic couplings, $L_{\sigma S}$ – dissipation inductance of stator windings, $L_{\sigma RL}$ – dissipation inductance of
tooth-end face dissipation of the rotor, transforming the system from transformed currents to t=hase curents, the mathematical model of the electromechanical system was obtained:

$$\frac{d\mathbf{i}_S}{dt} = \mathbf{A}_S(\mathbf{u}_S - \mathbf{r}_S\mathbf{i}_S) + \mathbf{A}_{SR}(-\mathbf{u}_R - \mathbf{\Omega\Psi}_R - \mathbf{r}_{RL}\mathbf{i}_R) \,; \tag{11}$$

$$\frac{d\mathbf{i}_R}{dt} = \mathbf{A}_{RS}(\mathbf{u}_S - \mathbf{r}_S\mathbf{i}_S) +$$

$$+\mathbf{A}_R(-\mathbf{u}_R - \mathbf{\Omega\Psi}_R - \mathbf{r}_{RL}\mathbf{i}_R) + \mathbf{\Omega}\mathbf{i}_R \,; \tag{12}$$

$$\frac{\partial^2 \varphi}{\partial t^2} = \frac{G}{\rho}\frac{\partial^2 \varphi}{\partial x^2} + \frac{\xi}{\rho J_p}\frac{\partial^3 \varphi}{\partial x^2 \partial t} \,, \tag{13}$$

where:

$$\begin{bmatrix} i_A & i_B \end{bmatrix}^{\mathrm{T}} = \begin{bmatrix} i_{SA} & i_{SB} \end{bmatrix}^{\mathrm{T}} + \mathbf{\Pi}\begin{bmatrix} i_{RA} & i_{RB} \end{bmatrix}^{\mathrm{T}} = \begin{bmatrix} i_{SA} & i_{SB} \end{bmatrix}^{\mathrm{T}} +$$

$$+\begin{bmatrix} i_{RA}^{\Pi} & i_{RB}^{\Pi} \end{bmatrix}^{\mathrm{T}}, \ \tau = \frac{1}{L_m} = \left(\frac{\psi_m}{i_m}\right)^{-1}; \ \rho = \left(\frac{\partial \psi_m}{\partial i_m}\right)^{-1}; \tag{14}$$

$$i_m = 2\sqrt{(i_A^2 + i_A i_B + i_B^2)/3} \,, \qquad b = \frac{2}{3}\frac{R - B}{i_m^2} \,; \tag{15}$$

$$\psi_m = 2\sqrt{(\psi_A^2 + \psi_A\psi_B + \psi_B^2)/3} \,, \ b_A = b(2i_A + i_B) \,; \tag{16}$$

$$B = 1/(\alpha_{\sigma S} + \alpha_{\sigma RL} + \tau) \,, \quad 1/(\alpha_{\sigma S} + \alpha_{\sigma RL} + \rho) \,; \tag{17}$$

$$b_B = b(2i_B + i_A) \,, \ \boldsymbol{\alpha}_{\sigma S} = \mathbf{L}_{\sigma S}^{-1} \,, \ \boldsymbol{\alpha}_{\sigma RL} = \mathbf{L}_{\sigma RL}^{-1} \,; \tag{18}$$

$$\mathbf{\Pi} = \frac{2}{\sqrt{3}}\begin{bmatrix} \sin(\varphi_1 + 120°) & -\sin\varphi_1 \\ \sin\varphi_1 & -\sin(\varphi_1 - 120°) \end{bmatrix}, \det \mathbf{\Pi} \neq 0 \,; \tag{19}$$

$$\mathbf{\Omega} = \mathbf{\Pi}\frac{d\mathbf{\Pi}^{-1}}{dt} \equiv \frac{d\mathbf{\Pi}^{-1}}{dt}\mathbf{\Pi} \equiv -\mathbf{\Pi}^{-1}\frac{d\mathbf{\Pi}}{dt} = \frac{\omega_1}{\sqrt{3}}\begin{bmatrix} 1 & 2 \\ -2 & -1 \end{bmatrix}; \tag{20}$$

$$\mathbf{G}_S = \boldsymbol{\alpha}_{\sigma S}\mathbf{G}, \mathbf{G}_R = \boldsymbol{\alpha}_{\sigma RL}\mathbf{G\Pi}, \mathbf{G} = \begin{bmatrix} B + b_A i_A & b_B i_A \\ b_A i_B & B + b_B i_B \end{bmatrix}; \tag{21}$$

$$\mathbf{A}_S = \boldsymbol{\alpha}_{\sigma S}(\mathbf{1} - \boldsymbol{\alpha}_{\sigma S}\mathbf{G}), \ \mathbf{A}_{SR} = -\boldsymbol{\alpha}_{\sigma S}\boldsymbol{\alpha}_{\sigma RL}\mathbf{G\Pi} \,; \tag{22}$$

$$\mathbf{A}_{RS} = -\mathbf{\Pi}^{-1}\boldsymbol{\alpha}_{\sigma S}\boldsymbol{\alpha}_{\sigma RL}\mathbf{G}, \ \mathbf{A}_R = \mathbf{\Pi}^{-1}\boldsymbol{\alpha}_{\sigma RL}(\mathbf{1} - \boldsymbol{\alpha}_{\sigma RL}\mathbf{G})\mathbf{\Pi} \,. \tag{23}$$

The electromagnetic moment of the motor is described with the relationship [1]

$$M_E = \sqrt{3} p_0 (i_{SB} i_{RA}^{\Pi} - i_{SA} i_{RB}^{\Pi})/\tau \,. \tag{24}$$

The voltage in the rotor cage bars was determined from the equations of magnetic field [1]:

$$\frac{\partial H_j}{\partial t} = \frac{\nu}{\gamma}\frac{\partial^2 H_j}{\partial z^2}, \ E_j = -\frac{k_u k_i}{\gamma}\frac{\partial H_j}{\partial z}, \quad j = A, B \tag{25}$$

with the boundary conditions [1]:

$$H_j\big|_{z=0} = \frac{i_{R,j}}{a}, \ H_j\big|_{z=h} = 0 \,, \quad j = A, B \,, \tag{26}$$

where H – component of magnetic field strength along z axis, k_u, k_i – transformation coefficients for the motor with respect to voltage and current, respectively, ν –magnetic reluctivity of the wire in the rotor slot, γ – electri conductivity of the wire in the rotor slot, a – zone of slot uncovering

Carrying out the spatial disceptization of the equation (24) taking into account (25) the equations with ordinary derivatives in the normal Cauchy form were obtained [2, 3]

$$\frac{dH_{j,k}}{dt} = \frac{\nu}{\gamma(\Delta z)^2}(H_{j,k-1} - 2H_{j,k} + H_{j,k+1}), \ j = A, B \,, \tag{27}$$

where k – number of the discretization unit, ($k \geq 10$),

The sought voltage is given with (28):

$$u_{R,j} = -l\frac{k_u k_i}{2\gamma\Delta z}(-3H_{j,1} + 4H_{j,2} - H_{j,3}), \ j = A, B \,, \tag{28}$$

The equations (13) take real sense only when they take into account boundary and initial conditions, i.e search for the motion of the mechanical system leads in the mathematical sense to a solution of a mixed problem. Of course initial conditions are preset, and the main problem is to solve the mixed problem and finding boundary conditions. These conditions were determined from the d'Alambert principle, i.e. moment equilibrium equations on the shaft boundaries. So, for the left and the right integration boundaries, the boundary conditions are given with the relationships:

(29) $$J_R \frac{d\omega_1}{dt} - GJ_p \frac{\partial \varphi}{\partial x} - \xi \frac{\partial^2 \varphi}{\partial x \partial t} = M_{EM} ;$$

(30) $$GJ_p \frac{\partial \varphi}{\partial x} + \xi \frac{\partial^2 \varphi}{\partial x \partial t} - J_\Sigma \frac{d\omega_{90}}{dt} = M_\Sigma .$$

Successive discreetized equations with respect to Fig. 1.

$$\frac{\partial^2 \varphi_i}{\partial t^2} \equiv \frac{\partial \omega_i}{\partial t} = \frac{G}{\rho} \frac{\varphi_{i-1} - 2\varphi_i + \varphi_{i+1}}{(\Delta x)^2} +$$

(31) $$+ \frac{\xi}{\rho J_p} \frac{\omega_{i-1} - 2\omega_i + \omega_{i+1}}{(\Delta x)^2}, \quad i = 1,2,...,90 ;$$

Discretizing the boundary conditions (29), (30), the following relationships were obtained:

(32) $$J_R \frac{d\omega_1}{dt} - GJ_p \frac{\varphi_2 - \varphi_0}{2\Delta x} - \xi \frac{\omega_2 - \omega_0}{2\Delta x} = M_{EM} ;$$

(33) $$GJ_p \frac{\varphi_{91} - \varphi_{89}}{2\Delta x} + \xi \frac{\omega_{91} - \omega_{89}}{2\Delta x} - J_\Sigma \frac{d\omega_{90}}{dt} = M(\omega_{90}) .$$

Solving together the equations (31) – (33):

(34) $$\frac{d\omega_1}{dt} = \frac{2\left(M_{EM}\Delta x - J_p G(\varphi_1 - \varphi_2) - \xi(\omega_1 - \omega_2)\right)}{\left(J_p \rho \Delta x + 2J_R\right)\Delta x} ;$$

(35) $$\frac{d\omega_i}{dt} = \frac{G}{\rho} \frac{\varphi_{i-1} - 2\varphi_i + \varphi_{i+1}}{(\Delta x)^2} + \frac{\xi}{\rho J_p} \frac{\omega_{i-1} - 2\omega_i + \omega_{i+1}}{(\Delta x)^2} ,$$

where $i = 2, 3...,89$.

(36) $$\frac{d\omega_{90}}{dt} = \frac{2\left(-M_\Sigma \Delta x + J_p G(\varphi_{89} - \varphi_{90}) + \xi(\omega_{89} - \omega_{90})\right)}{\left(J_p \rho \Delta x + 2J_\Sigma\right)\Delta x} .$$

(36) $$\frac{d\varphi_i}{dt} = \omega_i, \quad i = 1,2,...,90 .$$

The system of differential equations (11), (12), (27),(34) – (37) is subject to integration, taking into account (14) – (26), (28).

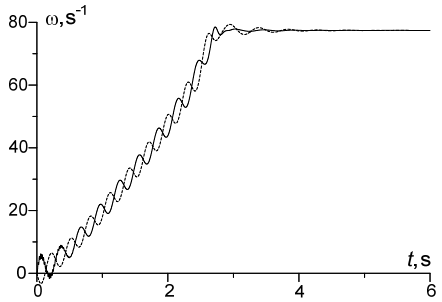

Fig. 2. Transient time dependencies of angular velocities of the rotor (continuous line) and the drive mechanism (broken line)

Results of computer simulations.

For transient analysis a deep slot asynchronous drive, whose graph is depicted in Figure 1, has been applied. The nominal data for the motor: P_H = 320 kW; U_H = 6 kV; I_H = 39 A; $\omega_H = 740$ s^{-1}, p_0 = 4, J_R = 49 kg·m^2 and parameters r_S = 1,27 Ω, R_{RL} = 0,21 Ω, α_S = 38,9 H^{-1}, α_{RL} = 70 H^{-1}, h = 0,038 m, l = 0,23 m, a = 0,005 m, J_Σ = 49 kg·m^2. The magnetization curve of the motor is given with the equation: $\psi_m = 12,4 \operatorname{arctg}(0,066 i_m)$. The parameters of long shaft are: $G = 8,1 \cdot 10^{10}$ N·m, $\rho = 7850$ Kg/m^3, $d = 0,05$ m, $L = 4,45$ m, $\xi = 0,5$ N·m^2·s, $\Delta x = 0,05$ m.

In Fig. 2 the dependencies of rotational velocity of the rotor (solid line) and drive mechanism (dashed line) are presented as functions of time. Analyzing these two curves one can notice a substantial difference between them. Oscillations of both processes are almost inverted by 180 deg. In Figs. 3 and 4 the transient currents of phase A of the stator are shown. In Fig. 3 the current in the examined system is depicted, whereas in Fig. 4 the same current is shown, but for ideally stiff shaft. From the comparison we can draw a conclusion about a strong coupling of electromagnetic and mechanical fields, i.e that mechanical wave transforms into electromagnetic one and vice versa.

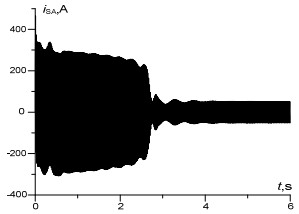

Fig. 3. Current of phase *A* of the stator as the function of time for the elastic shaft

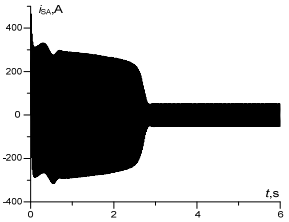

Fig. 4. Current of phase *A* of the stator as the function of time for an absolutely stiff shaft

In Fig. 5 a dependence of elasticity moment in the shaft line versus time between the discretization nodes 1 and 2 is depicted. In this Figure the frequency of oscillations of shaft line may be read.

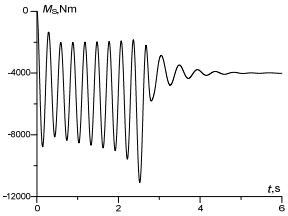

Fig. 5. Elasticity moment in the shaft line between discretization nodes 1 and 2

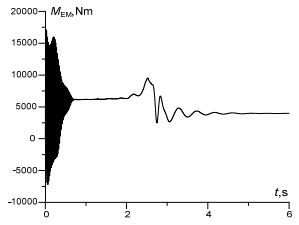

Fig. 6. Start-up moment of the asynchronous moment versus time

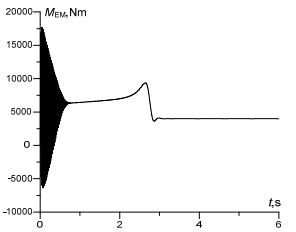

Fig. 7. Start-up moment of the asynchronous moment versus time

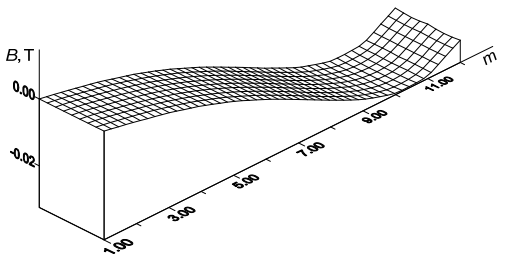

Fig. 8. Spatial distribution of in the slot

Figs. 6 and 7 depict transient start-up moments of the drive motor. In Fig. 6 the moment is shown for the examine motor, whereas in Fig. 7 for the non-elastic system. The physical processes are similar to those from Figs. 3 and 4. Here the principles of electromechanical energy transformations are also visible.

Figs. 8 and 9 present the spatial distribution of induction in a deep slot of the asynchronous for two cases considered, i.e. for the elastic system and for the stiff system. From the Figures it follows that there are different induction distributions then, what validates the well-known concept of electromechanical energy transformation on the level of electromagnetic and mechanical fields.

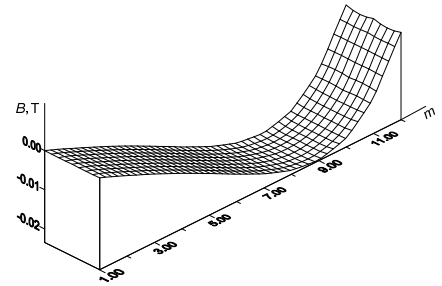

Fig. 9. Spatial distribution of induction in the slot for absolutely stiff shaft line

In Fig. 10 a spatial-temporal distribution of rotation velocity of the shaft line in the range $t \in [0;\ 0,6]$ s is shown.

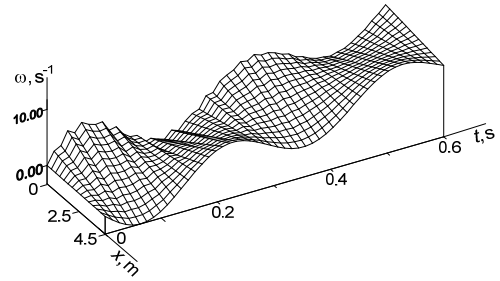

Fig. 10. Spatial-temporal distribution of rotational velocity for $t \in [0;\ 0,6]$ s

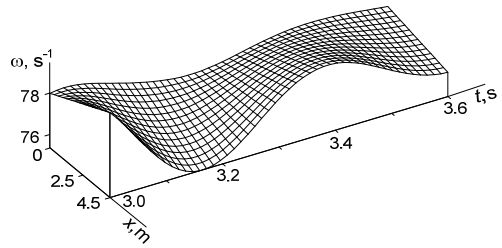

Fig. 11. Spatial-temporal distribution of rotational velocity for $t \in [3,0;\ 3,6]$ s

In Fig. 12 the same dependence is shown, as in Fig. 11, but for time range: $t \in [3,0;\ 3,6]$ s.

Conclusions

The application of novel interdisciplinary method presented in [1] made it possible to develop a mathematical model of rather complex drive system consisting of a deep slot asynchronous motor and a long elastic shaft, avoiding the decomposition of homogenous electromechanical system.

By means of computer simulations realistic depictions of movements of elastic wave along shaft and its influence on electromechanical wave in the rotor slot and vice versa have been obtained. It was possible only by the use of a composition of mathematical models of a deep slot induction motor and long shaft obtained from variational principles.

A combination of ordinary differential equations and partial differential equations in a single system makes it possible to describe complicated processes from the physical principles resulting from the least action rule [1, 4].

REFERENCES

[1] Chaban A. Modelowanie matematyczne procesów oscylacyjnych systemów elektromechanicznych. (Wydanie drugie, zmienione i uzupełnione), Lwów, Wyd. T. Soroki 2008 (w języku ukraińskim).

[2] Kharchenko E. Procesy dynamiczne w maszynach górniczych, Lwów, Sweet, 1991 (w języku rosyjskim)

[3] A. Rusek, A. Czaban, M. Lis Modelowanie matematyczne procesów oscylacyjnych w linii wałów o parametrach rozłożonych // Technical News . – 2011/1(33), 2(34). – S. 66 – 68.

[4] Ortega R., Loria A., Nicklasson P.J., Sira-Ramirez H. Passivity-Beast Control of Euler-Lagrange Systems: Mechanical, Electrical and Electromechanical Applications. London: Springer Verlag, 1998

[5] Timoszenko S., Young D., Weaver W. Drgania w sprawie inżynierowej. – Moskwa.: Maszynoznawstwo, 1985 (w języku rosyjskim).

[6] Ziemiński R. Analiza drgań swobodnych pełnego układu dyskretno-ciągłego typu // Zesz. Nauk. A.G.H. – 1980. – № 775. – S. 177 – 188.

***Autorzy**: prof. nadzw., dr hab. inż. Andriy Czaban, Politechnika Częstochowska, Wydział Elektryczny, al. Armii Krajowej 17, oraz Politechnika Lwowska, katedra mechaniki i automatyzacji budowy maszyn, ul Bandery 12, Lwów, Ukraina, E-mail: atchaban@gmail.com; dr. inż. Marek Lis, Politechnika Częstochowska, Wydział Elektryczny, al. Armii Krajowej 17, E-mail: lism@el. pcz.czest.pl.*